Gravitational Wave Spin Memory Effect and Detectability with LISA

Yara Yousef
Advisor: David Nichols

[1] *Astronomy and Physics Departments*
University of Virginia
Charlottesville, VA 22904

ABSTRACT

The Laser Interferometer Space Antenna (LISA) is a space-based gravitational wave observatory currently projected to launch in the 2030s. Its frequency range will be lower and broader than LIGO's, allowing it the capability to observe mergers and events we have still been unable to detect. Its increased sensitivity also allows for the potential to observe other effects of gravitational waves, such as gravitational wave memory. The memory effect we are focused on in this project is called the spin memory effect, which arises from the flux of the angular momentum per solid angle of the gravitational wave. This paper discusses gravitational wave memory and its derivation, the noise curve model for LISA, and the computation of the signal-to-noise ratios of detections. Our results for the spin memory ($l = 3, m = 0$) mode are not yet ready for publication, however the preliminary results for the pre-translation $l = 2, m = 2$ mode have been included.

1. INTRODUCTION TO GRAVITATIONAL WAVES

Gravitational waves are ripples in spacetime that propagate at the speed of light. While they can technically be produced by any object in non spherically or rotationally symmetric motion involving changes in acceleration, the radiation is extremely small unless it originates in regions of strong and dynamic gravitational fields. One such source is a compact binary, for example binary black holes or neutron stars. Gravitational waves carry off orbital energy, eventually leading to the merger of the two objects. The waves propagate out from the source in all directions, and contain information about both the source and its environment.

Gravitational waves were first detected in September of 2015 when a binary black hole merger (GW150914) was observed by the Laser Interferometer Gravitational-Wave Observatory (LIGO) sites in Hanford, Washington and Livingston, Louisiana (1). The event data matched the predictions of general relativity for the inward spiral, coalescence, and ringdown of the resultant black hole, and confirmed the existence of stellar mass black hole binaries.

The amplitude of gravitational waves is most commonly described using the dimensionless parameter

$$h = \frac{2\Delta d}{d} \tag{1}$$

where d is the displacement, or the characteristic distance between two points, and Δd is the change in that distance between them as a wave passes by. Therefore, the strain h is a measure of the fractional change in the proper distance between two points as a result of a gravitational wave.

This project focuses on the asymptotic gravitational waveform of the Bondi framework [1 2], which uses the set of coordinates (u, r, θ^A), where $u = t - r$ is the retarded time, r is an affine parameter[3] along outgoing (from the source) null rays, and θ^A are arbitrary coordinates on the 2-sphere[4].

Specifically, within the post-Newtonian-expanded, multipolar post-Minkowski approximation (or simply the PN approximation). Thus, the gravitational

[1] A formalism of General Relativity in which the coordinates are adjusted to the spacetime's null geodesics.[2]

[2] A null geodesic is one whose interval equals zero and has no proper time associated with it. It is the path that massless particles, such as photons, follow.

[3] A parameter on a curve which is preserved under the fundamental group of transformations of the affine space.

[4] The two-dimensional surface of a three-dimensional ball in three-dimensional space.

waveform is encoded within a symmetric, trace-free, and transverse tensor (11)

$$h_{ij}^{\mathrm{TT}} = \frac{1}{r}\sum_{m,l\geq 2}[U_{lm}(u)T_{ij}^{(e),lm} + V_{lm}(u)T_{ij}^{(b),lm}] + O(1/r^2) \tag{2}$$

where r is the distance from the source to the detector, u is the retarded time, $T_{ij}^{(e),lm}$ and $T_{ij}^{(b),lm}$ are tensor harmonics, $U_{lm}(u)$ are the radiative mass moments, and $V_{lm}(u)$ and the radiative current moments.

$U_{lm}(u)$ and $V_{lm}(u)$ can be related to the complex waveform

$$h = h_+ - ih_\times \tag{3}$$

using the spin-weighted spherical-harmonic expansion

$$h = \sum_{l,m} h_{lm}(u)_{-2}Y_{lm} \tag{4}$$

where

$$h_{lm} = \frac{1}{r\sqrt{2}}(U_{lm} - iV_{lm}) \tag{5}$$

2. GRAVITATIONAL WAVE MEMORY

Since it has been confirmed that gravitational waves exist at all, and since upgrades to LIGO have significantly improved its sensitivity, some focus is shifting back to the physical effects of rippling spacetime. One such effect is gravitational wave memory.

Gravitational waves distort the shape of spacetime, which results in a change of relative positions, velocities, accelerations, and trajectories of freely falling observers. The idea of gravitational wave memory postulates that spacetime does not simply return to its original state after a wave has passed, instead "remembering" it in that the proper distances between objects is permanently changed, even after the oscillations have ceased. For example, assume the arms of LIGO are the exact same length to start. After a wave passes, the x-arm may then be longer than the y-arm, or vice versa. The effect can be visualized with freely falling masses as shown in Figure (1).

Gravitational wave memory can also be seen in its effect on the wave strain, as shown in Figure (2).

The standard gravitational wave memory effect, referred to as displacement memory, arises from the energy carrying gravitational waves. It is produced by isolated sources that asymmetrically radiate energy density in massless, or gravitational, fields, or by sources that have changes in supermomentum charges

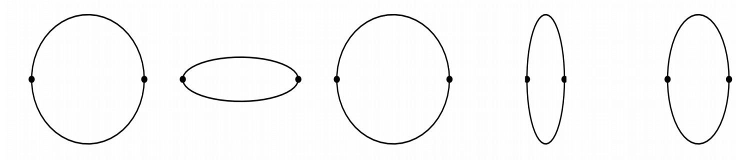

Figure 1: Image source: (9). A representation of the gravitational wave memory effect using a ring of freely falling masses, with time moving from left to right. The first frame shows the two particles relative to each other before a gravitational wave passes. The next three frames shows the two particles relative positions oscillating as a wave passes. The change in displacement occurs in the transverse plane to the radiation, causing a stretch alone one axis then a squeeze in the orthogonal axis. The final frame shows the particles after the wave has passed entirely, with their relative positions permanently changed.

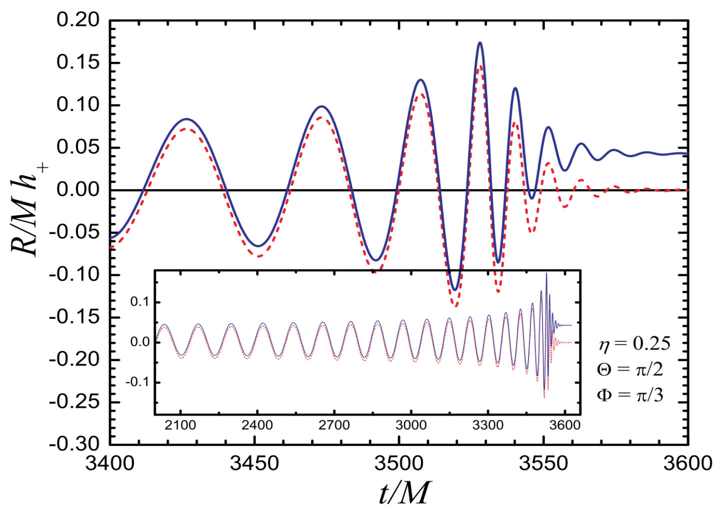

Figure 2: Image source: (5). The gravitational wave strain of an equal mass binary black hole merger event. The blue line represents the $h+$ polarization of the strain with the effects of gravitational wave memory included. The red dashed line represents the $h+$ polarization without the effect.

(11). Secondary waves are produced, leading to a constant offset of the waveform. This effect has small contributions from the early stages of the inspiral but grows more rapidly the more relativistic the binary. A formula for "practical computations" of the memory was given by Kip Thorne (14) as

$$h_{mem}(t) = \frac{2}{r}\int_{-\infty}^{t} dt' \int d\Omega' \frac{d^2E}{dt'd\Omega'}(1+\cos\theta')e^{2i\phi'} \tag{6}$$

where t is some time after the wave has passed, $d\Omega'$ is the solid angle, and

$$\frac{d^2E}{dt'd\Omega'} \tag{7}$$

is the gravitational wave flux. This integrates over the entire history of the wave up to the current time. Memory effects are larger for edge-on systems, as opposed to the primary oscillatory wave, which is strongest from face-on systems. To see this effect, an event with a signal-to-noise ratio (SNR) of about 100 is necessary.

For reference, the loudest event detected by LIGO thus far had an SNR of about 30.

3. SPIN MEMORY EFFECT

Another type of gravitational wave memory effect is spin memory, which is the form of the effect we are concerned with for the sake of this project. The spin memory effect is produced by asymmetric changes in angular momentum per unit solid angle to null infinity in massless fields (11). It is also produced by changes in superspin charges, the magnetic-parity part of the charges conjugate to the super-rotation vector fields. This results in an offset in the time integral in the gravitational wave strain, producing an extra pulse, as shown in Figure (3).

The spin memory effect gradually accumulates over the inspiral of the binary merger to have a significant effect. The leading order effect for non-spinning binaries is found in the $l = 3$, $m = 0$ spin-weighted spherical harmonic mode of the wave strain, aptly named the "spin memory mode".

3.1. *Relation of the Spin Memory Mode to Radiative Moments*

This section is an overview of how the spin memory mode is derived in terms of the radiative mass quadrupole moments. First, the shear tensor[5], also symmetric and trace-free, can be written as the sum of two terms, the first being electric parity and the second being magnetic parity,

$$C_{AB} = \frac{1}{2}(2D_AD_B - h_{AB}D^2)\Phi + \epsilon_{C(A}D_{B)}D^C\Psi \tag{8}$$

where h_{AB} is the metric on a round 2-sphere, D_A is the covariant derivative compatible with h_{AB}, and ϵ is the antisymmetric (Levi-Civita) tensor on a 2-sphere. Φ and Ψ are smooth functions of coordinates (u, θ^A), with Φ being the displacement memory observable. The spin memory observable is defined as

$$\Delta\Sigma \equiv \int du\Psi \tag{9}$$

$\Delta\Sigma$ is determined by changes in the angular momentum flux per unit solid angle in matter and gravitational waves, as well as changes in the curl of $\Delta\hat{N}_A$, a quantity which is a generalization of the spin of the system, or the superspin charges (11).

For non-spinning, quasicircular compact binaries in the PN approximation, with the orbital angular momentum along the z axis, the only relevant multipoles at leading order are $U_{2,2}$ and $\dot{U}_{2,-2}$ and their complex conjugates. The only relevant moment at leading order of the spin memory will be the $l = 3$, $m = 0$ mode, as all others will be higher order PN quantities. Therefore, $\Delta\Sigma$ becomes

$$\Delta\Sigma = \frac{1}{80\sqrt{7\pi}}Y_{3,0}\int_{-\infty}^{u_f} du\Im(\bar{U}_{2,2}\dot{U}_{2,2}) + O(c^{-2}) \tag{10}$$

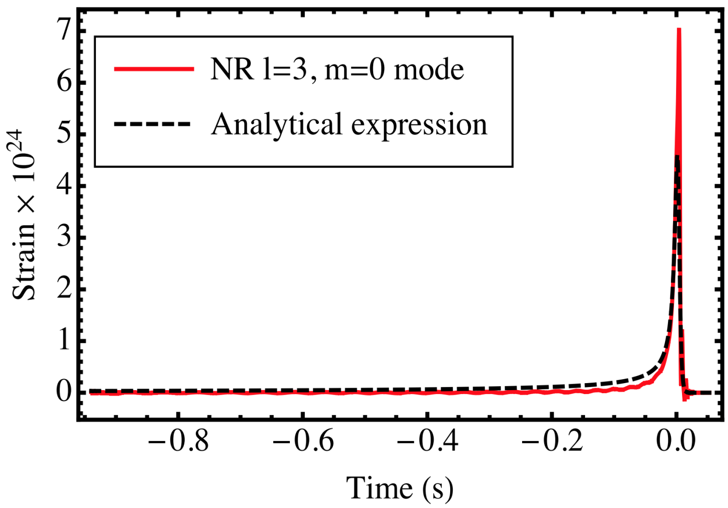

Figure 3: Image source: (11). The gravitational wave strain shown in (3,0) mode, or the spin memory mode. The red line shows the spin memory mode in a numerical relativity simulation. The black dashed line shows the spin memory mode computed from the $l = 2$, $m = \pm 2$ modes using the associated analytical expression. The waveform is scaled to have parameters like that of the GW150914 event.

[5] Part of the stress-energy tensor: the components T^{ik} where $i \neq k$ represent shear stress.

where $U_{lm}(u)$, the radiative mass quadrupole moments, can be solved for using Eq. (5) to get

$$U_{2,2} = r\sqrt{2}h_{2,2} \tag{11}$$

If we plug in the explicit expression for the spin-weighted spherical harmonic and evaluate the integral in Eq. (10), we find

$$h_{\times}^{\mathrm{smm}} = \frac{3}{64\pi r}\Im(\bar{U}_{2,2}\dot{U}_{2,2})\sin(\theta)^2\cos(\theta) \tag{12}$$

denoted the "spin memory mode" due to its close connection to the spin memory.

3.2. *Compact Binaries in the PN Approximation*

While equations (11) and (12) are valid for any $U_{2,2}$, it also useful to look at the derivation for a more specific form of the spin memory mode: that of compact binaries in quasicircular orbits, for which

$$U_{2,2} = -8\sqrt{\frac{2\pi}{5}}\eta M x e^{ix^{-5/2}/16\eta} + O(c^{-2}) \tag{13}$$

and

$$\dot{U}_{2,2} = 16i\sqrt{\frac{2\pi}{5}}\eta x^{5/2} e^{ix^{5/2}/16\eta} + O(c^{-2}) \tag{14}$$

where $M = m_1 + m_2$ is the total mass of the system with m_1 and m_2 being the individual masses of the two binary objects, $\eta = m_1 m_2/M^2$ is the symmetric mass ratio, and x is the PN parameter, given by $x = M/r$ for circular orbits.

We return to the integral in Eq. (10) and evaluate it by transforming the coordinate to x. We make the assumption that the binary formed at a finite separation, or that as $u \to -\infty$, x approaches $x_{-\infty}$, a small but nonzero value. $\Delta\Sigma_{3,0}$ is then

$$\Delta\Sigma = \frac{1}{10}\sqrt{\frac{\pi}{7}}\eta M^2(x_f^{-1/2} - x_{-\infty}^{-1/2})Y_{3,0} + O(c^{-2}) \tag{15}$$

When we take the u integral of the magnetic-parity part of the shear tensor C_{AB} from Eq. (8) we find

$$\epsilon_{C(A}D_{B)}D^C\Delta\Sigma = \sqrt{\frac{3\pi}{35}}\eta M^2(x_f^{-1/2} - x_{-\infty}^{-1/2})T_{AB}^{(b),3,0} \tag{16}$$

Looking at this, we can see the effect contributes to the u integral of the strain in the cross component

$$\int_{-\infty}^{u_f} du h_{\times}^{\mathrm{smm}} = \frac{1}{r}\sqrt{\frac{3\pi}{70}}\eta M^2(x_f^{-1/2} - x_{-\infty}^{-1/2})\,{}_{-2}Y_{3,0} + O(c^{-2}) \tag{17}$$

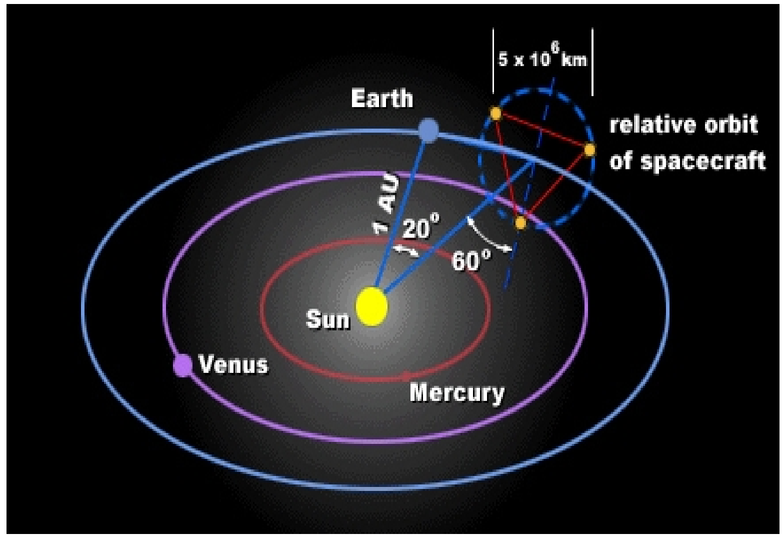

Figure 4: Image source: ESA (4). The schematic of LISA's orbit.

If we plug in the explicit expression for the spin-weighted spherical harmonic and differentiate the equation with respect to u, we find

$$h_{\times}^{\mathrm{smm}} = -\frac{12M\eta^2}{5r}x^{7/2}sin^2\theta cos\theta + O(c^{-2}) \tag{18}$$

4. LISA

As implied earlier, LIGO, for which the loudest event so far had an SNR of about 25 - 30, is simply not sensitive enough to realistically expect to observe gravitational wave memory effects for a single event. Hence, the need for future detectors. One of the upcoming gravitational wave observatories is the Laser Interferometer Space Antenna (LISA). This will be a space-based observatory: three spacecraft centered around a freely falling test mass, forming an equilateral triangle with arms extending about a million miles. It will be trailing tens of millions of miles behind Earth, more than 100 times the Earth-Moon distance. The schematic of LISA's orbit is shown in Figure (4). This observatory will have a lower and broader frequency range, about 10^{-4} - 1 Hz, than LIGO, which is about 10 - 1000 Hz, which means LISA has the potential to detect very loud events from supermassive binary mergers $10^5 - 10^7 M_\odot$. A noise sensitivity curve is shown in Figure (5), and a contour plot of constant SNR is shown in Figure (6).

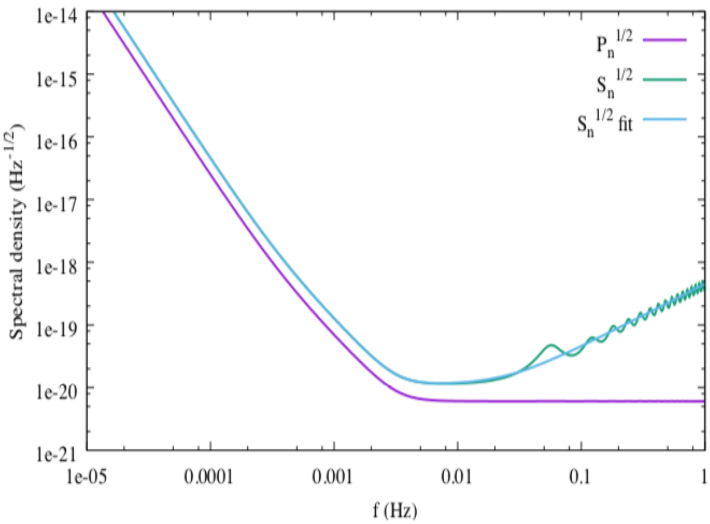

Figure 5: Image source: (13). The amplitude spectral density of the noise, and the corresponding sensitivity curve, found by dividing $P_n(f)$, the power spectral density of the detector noise, by $\mathcal{R}(f)$, the sky and polarization averaged signal response function of the instrument. The analytic fit to $S_n(f)$, the LISA sensitivity curve, is also shown.

4.1. *Noise Curve Model*

The sensitivity curve for LISA is well approximated by (13)

$$S_n(f) = \frac{10}{3L^2}\left(P_{OMS}(f) + \frac{4P_{acc}(f)}{(2\pi f)^4}\right)\left(1 + \frac{6}{10}\left(\frac{f}{f_*}\right)^2\right) + S_c(f) \quad (19)$$

where $L = 2.5$ Gm is the arm length, and $f_* = 19.09$ mHz $= c/L/2\pi$, or 1/2 the light travel time of the arms of the detector, divided by 2π. The expressions for $P_{OMS}(f)$, $P_{acc}(f)$, and $S_c(f)$ are given as follows.

P_{OMS} is the single-link optical metrology noise, which is the technical noise associated with the laser itself, arising between two of the observatory's detectors. It is given as

$$P_{OMS} = (1.5\times10^{-11}\mathrm{m})^2\left(1 + \left(\frac{2\mathrm{mHz}}{f}\right)^4\right)\mathrm{Hz}^{-1} \quad (20)$$

P_{acc}, the single test mass acceleration noise, is produced by the freely falling cube between the three spacecraft, which will use microthrusters to remain centered on it. This noise is defined as

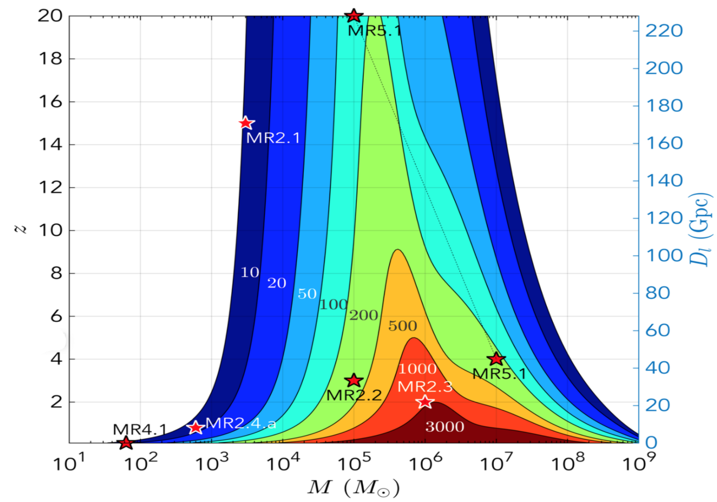

Figure 6: Image source: (3). Contours of constant SNR for the baseline LISA observatory in the plane of total source-frame mass M, redshift z (assuming Planck cosmology), and luminosity distance D_l for black hole binaries with a constant mass ratio of $q = 0.2$. The starred points mark the positions of the threshold binaries used to define the mission requirements.

$$P_{acc} = (3\times10^{-15}\mathrm{ms}^{-2})^2\left(1 + \left(\frac{0.4\mathrm{mHz}}{f}\right)^2\right)\left(1 + \left(\frac{f}{8\mathrm{mHz}}\right)^4\right)\mathrm{Hz}^{-1} \quad (21)$$

So the total noise in a Michelson-style LISA data channel is

$$P_n(f) = \frac{P_{OMS}}{L^2} + 2(1 + \cos^2(f/f_*))\frac{P_{acc}}{(2\pi f)^4 L^2} \quad (22)$$

$S_c(f)$ is called the Galactic confusion noise. On top of noise from the instrumentation, unresolved binaries in the galaxy will produce non-stationary noise. It's value decreases with mission time, as more foreground sources are removed (13). The estimate for the new LISA design is given as

$$S_c(f) = Af^{-7/3}e^{-f^{\alpha}+\beta f\sin(\kappa f)}[1+\tanh(\gamma(f_k - f))]\mathrm{Hz}^{-1} \quad (23)$$

where A is the amplitude, fixed to 9×10^{-45}, and α, β, κ, γ, and f_k[6] are parameters of the analytic fit that change with observation time. Their values at four different observation times are shown in Table 1.

[6] The knee frequency, an estimate of the maximum frequency component of the signal.

	6 months	1 year	2 years	4 years
α	0.133	0.171	0.165	0.138
β	243	292	299	-221
κ	482	1020	611	521
γ	912	1680	1340	1680
f_k	0.00258	0.00215	0.00173	0.00113

Table 1: Parameters of the analytic fit of the Galactic confusion noise. As observation time increases, the confusion noise drops off more steeply as a result of a decrease in f_k and an increase in γ.

5. SIGNAL-TO-NOISE RATIO

The signal-to-noise ratio (SNR) is a measure of the strength of a meaningful signal relative to that of the interference, or noise. The amplitude SNR for a deterministic signal $\tilde{h}(f)$ is defined by

$$\rho^2 = 4\int_0^\infty \frac{|\tilde{h}(f)|^2}{P_n(f)}df \tag{24}$$

where $\tilde{h}(f)$ is the Fourier transform of the detector response function

$$h(t) = F_+ h_+ + F_\times h_\times \tag{25}$$

where F_+ and $F_\times$ are the antenna response patterns of the detectors to the plus and cross polarizations of the waveform (11). Averaging over sky location, inclination, and polarization yields (13)

$$\bar{\rho}^2 = \frac{16}{5}\int \frac{fA^2(f)}{P_n(f)}d(\ln f) = \frac{16}{5}\int \frac{(2fT)S_h(f)}{S_n(f)}d(\ln f) \tag{26}$$

where T is observation time, $S_n(f)$ is the sensitivity curve, and $S_h(f)$ is the angle averaged, one-sided power spectral density of the signal

$$S_h(f) = \frac{A^2(f)}{2T} \tag{27}$$

It is this equation, in the form

$$\rho^2 = \frac{16}{5}\int_0^\infty \frac{|\tilde{h}(f)|}{S_n(f)}df, \tag{28}$$

that we use to calculate our SNRs for this project.

6. METHOD FOR COMPUTING THE SNRS OF MERGER MODELS

The model used in this project was taken from the "Binary black hole surrogate waveform catalog" (7), which holds the publicly available numerical relativity (NR) surrogate data for waveforms produced by the Spectral Einstein Code (SpEC)[7]. This surrogate model was for binary black hole systems with generic mass ratios and non-precessing spins. The NR waveform is hybridized with PN waveforms in order to include the early inspiral, then the surrogate is constructed.

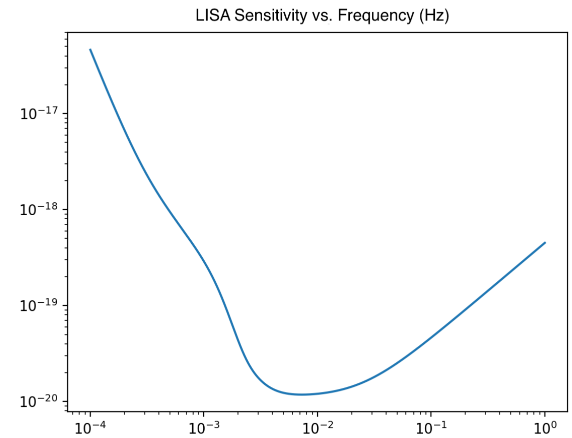

Figure 7: The LISA sensitivity vs. frequency curve computed with our code.

The GWSurrogate Python package (6) is then used to evaluate the surrogate model, and returns the (2,2) mode of the waveform. Since the surrogate model is not perfect, there is a certain amount of non-physical noise, especially towards the beginning of the waveform, associated with it. In order to reduce this noise, the wave strain is windowed using either a Tukey[8] or Planck window function. To refrain from cutting out important information from the end of the waveform (the merger and ringdown), the strain is padded at the end.

We then split the strain into its real and imaginary parts, and individually Fourier transform each using before adding them back together in quadrature to return to the full wave strain. We derive the LISA sensitivity curve $S_n(f)$ using Eq. (19) with an observation time T of four years. We then plug this curve and our previously derived strain into Eq. (28), in which the integral is evaluated using the Numpy trapz function (12).

[7] An infrastructure for solving partial differential equations using multi-domain spectral methods, designed for simulating compact objects with full general relativistic effects.

[8] A tapered cosine window.

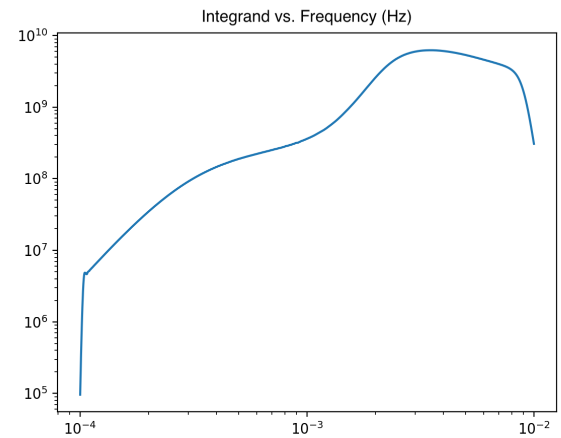

Figure 8: The SNR integrand vs. frequency curve.

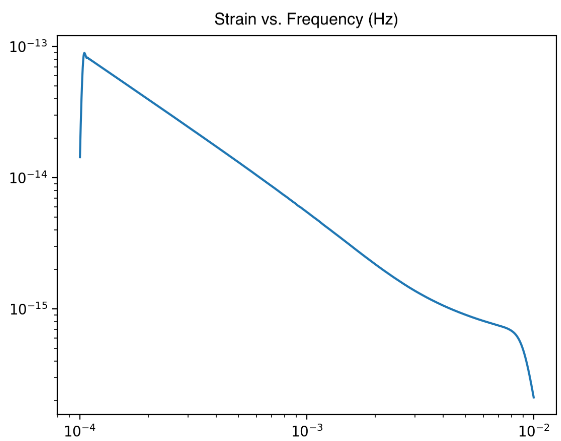

Figure 9: The wave strain vs. frequency curve.

We follow the same process when calculating the SNR for the (3,0) mode, the only difference being that we translate from the (2,2) mode evaluated by GWSurrogate using equations (11) and (12) before windowing the waveform.

The parameters of the model we are using for testing is a non-spinning binary with a mass ratio of $q = 1$, a total mass $M = 2 \times 10^6 M_{odot}$, an observation time $T = 4$ years, and is at a distance $D = 5$ Gpc. The following preliminary results were evaluated using a tukey window, implemented using the Scipy.signal package (16), with an alpha value $\alpha = 0.15$. The SNR of the (2,2) mode of this waveform was calculated using Eq. (28) to be SNR ≈ 10450. The sensitivity curve we computed using Eq. (19) is shown in Figure 7. The plots of the argument of the integral in Eq. (28) and that of the wave strain are shown in Figures 8 and 9.

REFERENCES

[1] Abbott, B. P., et al. (LIGO Scientific Collaboration and Virgo Collaboration) Observation of Gravitational Waves from a Binary Black Hole Merger. Physical Review Letters 116(6)

[2] Camp, J. B. and Cornish, N. J. Gravitational Wave Astronomy. Annual Review of Nuclear and Particle Science 54 (2004)

[3] Danzmann, K., et al. LISA: A proposal in response to the ESA call for L3 mission concepts.

[4] ESA. "Schematic of LISA's orbit", https://sci.esa.int/web/lisa/-/31704-schematic-of-lisa-orbit (Published: 2004, Last Updated: 2019)

[5] Favata, M. Gravitational-wave memory revisited: memory from the merger and recoil of binary black holes. Journal of Physics: Conference Series 154 (2009)

[6] Field, S., Galley, C., Hesthaven, J., Kaye, K., and Tiglio, M. Fast prediction and evaluation of gravitational waveforms using surrogate models. Physical Review X 4, 031006 (2014)

[7] Field, S. E., Galley, C. R., et al. Binary black-hole surrogate waveform catalog [Data set]. Zenodo (2019): http://doi.org/10.5281/zenodo.3629749

[8] Flanagan, E. E., Grant, A. M., Harte, A. I., Nichols, D. A. Persistent gravitational wave observables: General framework. Physical Review D 99(8)

[9] Johnson, A., Kapadia, S., Osborne, A., Hixon, A., and Kennefick, D. Prospects of Detecting the Nonlinear Gravitational Wave Memory. Physical Review D 99(4)

[10] Mädler, T. and Winicour, J. Bondi-Sachs Formalism. Scholarpedia 11, 33528 (2016)

[11] Nichols, D. Spin memory effect for compact binaries in the post-Newtonian approximation. Physical Review D 95(8)

[12] Oliphant., T. E. A guide to NumPy. Trelgol Publishing, USA (2006)

[13] Robson, T., Cornish, N. J., and Liu, C. The construction and use of LISA sensitivity curves. Classical and Quantum Gravity 36(10)

[14] Thorne, K. S. Gravitational-wave bursts with memory: The Christodoulou effect. Physical Review D 45(2)

[15] Thorne, K. S. Multipole expansions of gravitational radiation. Reviews of Modern Physics 52(2)

[16] Virtanen, P., et al. and SciPy 1.0 Contributors. SciPy 1.0: Fundamental Algorithms for Scientific Computing in Python. Nature Methods, in press (2020)